PHYSICAL REVIEW A, VOLUME 62, 011804(R)

Self-phase modulation and compression of few-optical-cycle pulses

V. P. Kalosha* and J. Herrmann
Max-Born-Institute for Nonlinear Optics and Short Pulse Spectroscopy, Max-Born-Straße 2a, D-12489 Berlin, Germany
(Received 8 October 1999; published 16 June 2000)

The nonlinear propagation of few-optical-cycle pulses through a dispersive Kerr medium, as, e.g., fused silica, is studied theoretically using a global approach to dispersion without applying the slowly varying envelope approximation. Contrary to amplitude self-steepening, a nearly triangular pulse shape with the steep side on the leading front is predicted. The calculation of the ultrawide spectrum and the spectral phases demonstrates that half-cycle pulses with a full width at half maximum as short as 0.5 fs and single-cycle pulses can be generated by the application of an appropriate broadband modulator for the compensation of the frequency-depending phase.

PACS number(s): 42.65.−k

Ever since its first observation, self-phase-modulation (SPM) of optical pulses due to a intensity-depending refractive index has attracted much interest, owing to its significance for a large variety of phenomena, such as spectral broadening or optical solitons (see, e.g., [1]). One of the most exciting applications is the utilization of SPM in a Kerr medium followed by propagation in a dispersive delay line for pulse compression [1–3]. By using this method recently, pulses with a duration of 4 to 5 fs at a center wavelength of 800 nm have been generated in single-mode fibers [4] and hollow fibers filled with noble gases [5]. The possibility of extending these ultrashort pulse sources into the optical subcycle regime is of considerable interest.

While the nonlinear propagation of pulses with a duration of many cycles in the dispersive Kerr medium is rather well studied (see, e.g., [1,3,6]), the physical phenomena in the ultrashort (few-cycle and subcycle) regime are not yet well understood. In this region widely used approximate methods, such as a truncated Taylor series approximation to dispersion and the slowly varying envelope approximation (SVEA), are no longer adequate to describe the pulse propagation. In the present Rapid Communication we solve the exact Maxwell equations without the use of the SVEA and apply a global approach to dispersion with a modified Sellmeyer expansion. In such a way dispersion effects, infrared losses due to vibrational modes as well as other higher-order effects as the intensity-depending group velocity are adequately taken into account. We study the temporal and spectral characteristics in the evolution of few-cycle pulses and the possibility of extending pulse shortening to the subcycle region. In other previous work on methods for sub-fs pulse generation, several alternatives has been studied, as high-harmonic generation with sub-fs time structure [7], cascaded stimulated Raman scattering [8] and pulse splitting by coherent propagation effects [9].

We consider the interaction of an ultrashort few-cycle pulse propagating in the z direction and linearly polarized in the x direction with a dispersive, nonresonant nonlinear optical material as fused silica. Through the influence of the incident field, a polarization in the medium is induced which can be separated into a linear (P_x^L) and a nonlinear part (P_x^{NL}): $P_x = P_x^L + P_x^{NL}$. The Fourier component for P_x^L is represented by $P_x^L(\omega,z) = \epsilon_0 \chi(\omega) E(\omega,z)$. The linear refractive index and linear loss measured for any optical materials in a wide spectral range can be modeled rather precisely by a modified Sellmeyer fit of the linear susceptibility as

$$\chi(\omega) = \sum_\ell S_\ell \left(\frac{1}{\omega_\ell - i\Gamma_\ell - \omega} + \frac{1}{\omega_\ell + i\Gamma_\ell + \omega} \right). \quad (1)$$

Equation (1) is the analog to the susceptibility of a linearized quantum multilevel system; here S_ℓ are the coefficients defined by matrix elements of the electronic ultraviolet (UV) and vibrational infrafred (IR) transitions, and ω_ℓ and Γ_ℓ are the resonance frequencies and the decay rates related to these transitions, respectively. Introducing the complex density matrix functions $\rho_\ell(t,z)$ by the relation $P_x^L(t,z) = \epsilon_0 \Sigma_\ell (\rho_\ell + \rho_\ell^*)$ we find from Eq. (1) in the time domain

$$\frac{\partial \rho_\ell}{\partial t} = (i\omega_\ell - \Gamma_\ell)\rho_\ell - iS_\ell E(t,z). \quad (2)$$

The nonlinear polarization far off medium resonance can be treated as a third-order process. Sheik-Bahae *et al*. developed a model for the dispersion of the dominant electronic part of $\chi^{(3)}$ for semiconductors and wide-gap optical solids that predicts a universal dispersion and scaling of $\chi^{(3)}$ in rather good agreement with measurements of many materials [10]. According to this model for $\omega \ll \omega_g$, where $E_g = \hbar\omega_g$ is the band-gap energy, the relation $\chi^{(3)}(\omega,\omega,-\omega,\omega) \approx \chi_0^{(3)}(1 + 2.8\omega^2/\omega_g^2)$ can be derived. For wide-gap materials, such as fused silica, $\tau_g = 1.67/\omega_g$ is about 0.05 fs, and consequently the second term in $\chi^{(3)}$ does not play a significant role even for subfemtosecond pulses considered here. With this model for the nonlinear polarization, $P_x^{NL}(t,z) = \epsilon_0 \chi_0^{(3)} E^3(t,z)$, describing the effects of SPM and self-steepening and also the generation of third harmonics, we can study the pulse propagation in the nonlinear medium by solving Maxwell's equations,

$$\frac{\partial B_y}{\partial t} = -\frac{\partial E_x}{\partial z}, \quad \frac{\partial D_x}{\partial t} = -\frac{\partial H_y}{\partial z}, \quad (3)$$

*Email address: kalosha@mbi-berlin.de

where $D_x=\epsilon_0 E_x+P_x$, $B_y=\mu_0 H_y$ and the electric field E_x and the magnetic field H_y are assumed uniform along the transverse x and y axes. The latter condition can be realized in waveguides. We choose the initial conditions as $E_x(0,z)=E_0\cos[\omega_0(z+z_0)/c]\mathrm{sech}[1.76(z+z_0)/c\tau_0]$ indicating that initially the pulse locates in vacuum at $z=-z_0$ before the medium entrance face at $z=0$; here E_0 is the peak strength of the electric field, ω_0 is the carrier frequency, τ_0 is the full width at half maximum (FWHM) of the pulse. Equations (2) and (3) were solved using the finite-difference time-domain method [11] with nonreflecting boundary conditions, the predictor-corrector method, and a moving computational domain. We studied pulse propagation in fused silica with characteristic dispersion parameters determined from the data in Ref. [12]. A suitable fit of the modified Sellmeyer formula (1) was achieved taking into account one IR resonance at $\omega_1=0.21$ fs^{-1} ($\lambda_1=9.05$ μm) with $S_1=0.06$ fs^{-1}, $\Gamma_1^{-1}=265$ fs; and one UV resonance at $\omega_2=18.9$ fs^{-1} ($\lambda_2=0.10$ μm) with $S_2=10.2$ fs^{-1}, $\Gamma_2=0$. Loss in the UV can be neglected because only the spectral region below ω_2 is considered. The third-order susceptibility is given by $\chi_0^{(3)}=(4/3)c\epsilon_0 n^2(\omega_0)n_2$ with $n_2=3\times10^{-16}$ cm^2/W, where $n(\omega_0)$ is the linear refractive index.

In order to obtain better insight into the specific characteristics of SPM in the few-optical cycle region, we first turn to the case of pulse propagation without taking the dispersion in the medium into account. We consider initial pulse parameters $\tau_0=5$ fs, $\lambda_0=0.83$ μm, $I_0=4\times10^{13}$ W/cm^2, and parameters for fused silica. The corresponding fluence of the initial pulse is one order below the damage threshold [13] and higher-order nonlinear effects are still negligible. Thus, the free-electron density due to photoionization and avalanche ionization can be estimated by $n<10^{16}$ cm^{-3}, which is in good agreement with experimental measurements and modeling in Ref. [13]. Then the plasma contribution to nonlinear refraction is three orders of magnitude smaller than the Kerr nonlinearity. In Fig. 1, pulse shape and spectrum and phase delay are presented after propagation of 0.1 mm. Owing to violation of the SVEA, the creation of new frequencies and their nonlinear mixing by the third-order nonlinearity in dispersionless medium is significantly increased in the few-cycle region and results in a dramatic shift of the spectrum into the UV region [solid curve in Fig. 1(b)]. A noteworthy feature is that the slow oscillations in the front of the pulse show a nonsinusoidal behavior with abrupt changes and dips in the maxima. The physical origin of such well-resolved carrier self-steepening can be explained by the action of the nonlinearity directly in the field strength. It is related to previously discussed carrier wave shocking [14] considered here at a propagation distance larger than the shock distance. The known effect of envelope self-steepening here is weak but still remarkable in the trailing edge [Fig. 1(a)]. The pulse is highly chirped as shown by the phase delay in Fig. 1(b) (dashed curve). For comparison, in the inset the spectrum is shown for the SVEA for the same distance, which qualitatively differs from the exact results and clearly demonstrates the failure of this approximation for few-optical-cycle pulses.

Figure 2 shows the evolution of the pulse with the same

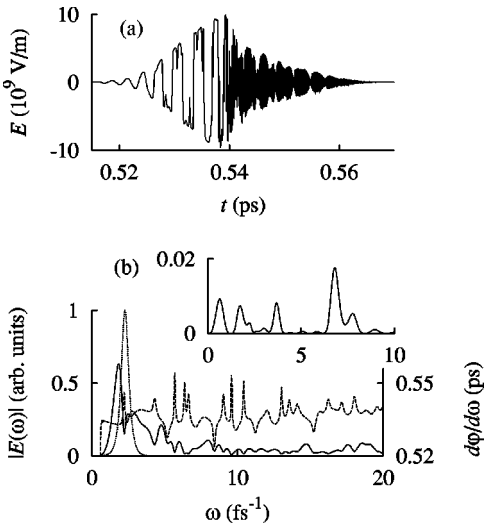

FIG. 1. (a) Pulse temporal shape and (b) spectrum (solid curve) and phase delay (dashed) at a distance $z=0.1$ mm of a dispersionless Kerr medium for the initial pulse duration $\tau_0=5$ fs, peak intensity $I_0=4\times10^{13}$ W/cm^2, and location $z_0=15$ μm. Dotted curve, initial pulse spectrum; inset, pulse spectrum for SVEA.

parameters, taking into account dispersion in silica. The above observed effect of carrier self-steepening does not occur because of the counteraction of dispersion. However, another interesting feature arises. As seen in Fig. 2 at a distance of 1 mm the pulse significantly spreads and develops a nearly triangular shape with the steep side on the pulse leading front. This behavior is contrary to the known effect of the envelope self-steepening for longer pulses with a steep front at the tailing edge. The triangular shape here is caused by the lower velocity of the high-frequency part of the spectrum for the normal-dispersive medium and, therefore, by self-flattening of the pulse back front. After the main pulse a weaker pulse can be seen that contains third-harmonic components and moves with a lower group velocity. In Fig. 3(a) the spectrum of the field $|E(\omega)|$ is shown for three propagation distances together with the initial pulse spectrum (dotted curve). In comparison with Fig. 1(b) the long tail on the blue side is now suppressed because of its lower group velocity,

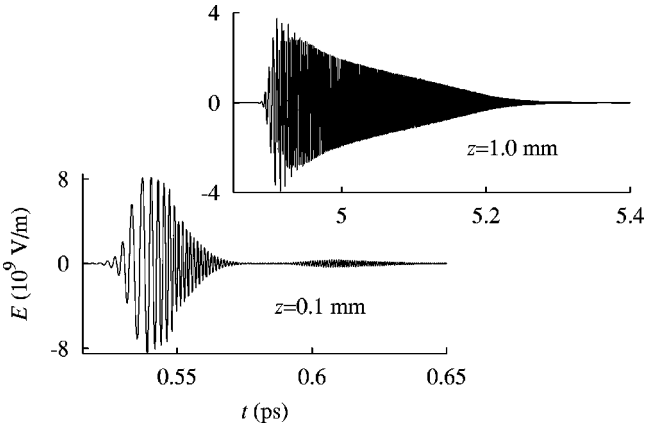

FIG. 2. Pulse shape in fused silica at $z=0.1$ and 1.0 mm for the same initial pulse parameters as in Fig. 1.

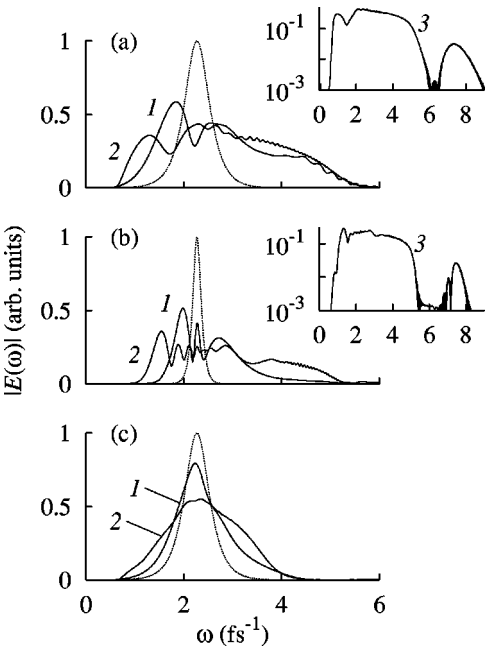

FIG. 3. Evolution of the pulse spectrum for different input pulse parameters and distances: (a) $\tau_0=5$ fs, $I_0=4\times10^{13}$ W/cm^2, $z=0$ (dotted curve), 0.1 (*1*), 0.5 (*2*), 1 mm (*3*, inset); (b) $\tau_0=15$ fs, $I_0=4\times10^{13}$ W/cm^2, $z=0$ (dotted), 0.1 (*1*), 0.5 (*2*), 1 mm (*3*, inset); (c) $\tau_0=5$ fs, $I_0=10^{13}$ W/cm^2, $z=0$ (dotted), 0.5 (*1*), 1 mm (*2*).

while only small changes occur in the spectral maximum on the red side. Nevertheless, the asymmetric double-peak spectrum is still extremely broad with a bandwidth of about $\Delta\approx1.7\omega_0$ exceeding the input carrier frequency ω_0. After propagation of 1 mm, the spectrum extends from $\lambda\approx3.0$ μm up to the UV $\lambda\approx0.3$ μm and remains unchanged during further propagation. In Fig. 3(b) the evolution of the spectrum for $\tau_0=15$ fs and $I_0=4\times10^{13}$ W/cm^2 is shown. Ultrawide spectral broadening sufficient for subcycle pulse generation can also be achieved for these input parameters and longer distances (curves *2* and *3*). In Fig. 3(c) the evolution of the spectrum for a weaker input pulse with $\tau_0=5$ fs and $I_0=10^{13}$ W/cm^2 is plotted for comparison. Now the maximum bandwidth $\Delta<\omega_0$ is smaller than in Figs. 3(a) and 3(b). In the insets of Figs. 3(a) and 3(b) the spectrum at $z=1$ mm is shown on a logarithmic scale for input pulses with $\tau_0=5$ and 15 fs, respectively. As can be seen, the spectrum of the third harmonics is shifted slightly towards higher frequencies because of the SPM-induced broadening of the fundamental. To compare our results with available experiments, note that an optical pulse compression up to 5 fs was reported [4] using spectral broadening in a single-mode fiber with pulse parameters at a focusing lens before the fiber close to those in Fig. 3(b). Besides the loss at the fiber entrance face, the pulse input parameters are considerably modified by chromatic and spherical aberrations of the lens, leading to significant temporal broadening of the short pulses [15], and therefore the predicted bandwidth in Fig. 3(b) with $\Delta\omega\approx3$ fs^{-1} is larger than reported in [4]. This is also supported by the results of Fork *et al.* [2], who have obtained

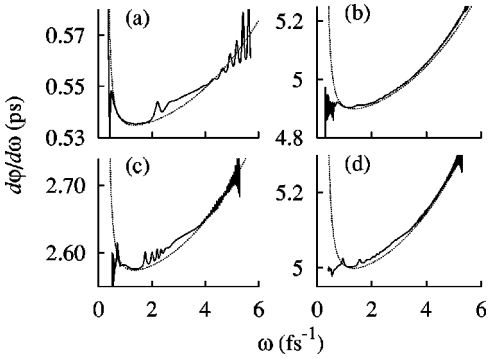

FIG. 4. Group delay at $z=0.1$ (a), 0.5 (c) and 1 mm (b),(d) for $\tau_0=5$ (a),(b) and 15 fs (c),(d), $I_0=4\times10^{13}$ W/cm^2. Dotted curves show the linear phase delay at the same distances and $z_0=15$ (a),(b), 45 μm (c),(d).

approximately the same spectrum bandwidth as in [4], but with 50-fs, 10^{12} W/cm^2 input pulses.

In Fig. 4 the group delay $d\varphi/d\omega$ of the pulse $E(\omega)=|E(\omega)|\exp[i\varphi(\omega)]$ is presented. For comparison, the corresponding linear phase delay $d\varphi_{lin}/d\omega$ with $\varphi_{lin}=\omega n(\omega)z/c+\omega z_0/c$ is depicted by the dotted lines. The group delay shows a smooth behavior in the main spectral part and only a small deviation from the linear phase delay for the smaller distance [Figs. 4(a) and 4(c)]. For the longer distance linear and nonlinear delay are almost identical [Figs. 4(b) and 4(d)]. The reason is that SPM plays a role only in the first step of the evolution when the pulse experiences a large spreading with decreasing pulse intensity; after that the change in the phase delay is dominated by linear dispersion.

The technique to compress highly modulated pulses (Figs. 2 and 3) consists of the utilization of anomalous dispersive optical elements for the compensation of the phase delay. The action of such an optical delay line (compressor) is described by a phase function $\varphi_c(\omega)$ and the Fourier-transformed field after the compressor is $E_c(\omega)=|E(\omega)|\exp[i\varphi(\omega)+i\varphi_c(\omega)]$. As the dotted curves of Figs. 5(a) and 5(b), the compressed pulses are shown after passage through an ideal compressor with $\varphi+\varphi_c=0$. They consist of almost half a cycle with two side-minima. The FWHM of pulse intensity $I_c(t)=2c\epsilon_0|E_c(t)|^2$ is only ≈0.5 fs, while the intensity level of the side wings is $\approx20\%$ of the maximum.

For pulses with an ultrawide spectrum considered here, usually applied techniques such as combinations of prism pairs and chirped mirrors [2–5] cannot be used for efficient pulse compression because of their restricted bandwidth. However, alternative methods have been demonstrated and are presently in progress. As an example, pulse shortening can be accomplished by spectrally dispersing the highly chirped pulses by a prism and focusing the spectrum onto a liquid-crystal spatial light modulator (LCSLM) [16,17]. Owing to pixellation the requirement for the largest pulse phase delay is given by $|d\varphi/d\omega|\ll\pi/\Delta\omega$ [16], where $\Delta\omega$ is the frequency space corresponding to a single pixel. We consider a typical transmission wavelength range between 0.4 and 1.8 μm; the spectral part outside this region is cut off. For the phase delay shown in Fig. 4(a) the above given condition is

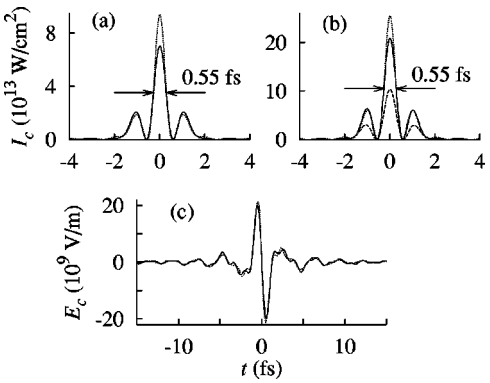

FIG. 5. Compressed pulses after propagation through 0.1 mm (a),(c) and 0.5 mm (b) of fused silica and after chirp compensation by a SLM for $\tau_0=5$ (a),(c), 15 fs (b), $I_0=4\times10^{13}$ W/cm^2, and different SLM parameters: (a) $N=256$, $\varphi_0=0$; (b) $N=1024$ (solid curve), 256 (dashed), $\varphi_0=0$; (c) $N=256$, $\varphi_0=\pi/2$. Corresponding pulses with chirp compensation by an ideal compressor are shown by the dotted curve.

well satisfied for the number of pixels $N=256$. The solid line in Fig. 5(a) shows the numerical result for compression by the LCSLM. As can be seen, the pulse duration of ≈0.55 fs and the obtained pulse shape are very close to those obtained with an ideal compressor. In Fig. 5(b) pulse shortening is shown for $\tau_0=15$ fs and $z=0.5$ mm by a LCSLM with $N=256$ (dashed curve) and $N=1024$ pixels (solid curve). Note that SLM also permits the control of the absolute value of the resultant phase $[\varphi(\omega)+\varphi_c(\omega)=\varphi_0,\ \varphi_0=\text{const}]$. Its crucial role can be seen in Fig. 5(c), where the electric field of the single-cycle pulse for $\varphi_0=\pi/2$ is completely different from the case of the half-cycle pulse in Fig. 5(a) with $\varphi_0=0$ after passage through the ideal (dotted curve) as well as the real compressor with $N=256$ pixels (solid curve). Though both pulses have identical spectral intensity distributions, striking differences in the nonlinear interaction of these pulses with matter are to be expected.

LCSLM's have been used for pulse shortening down to 13 fs [17] and no obvious factors limiting the extension to shorter pulses have been identified up to now [16]. The application of this method to a ten times broader spectrum could lead to difficulties, but obtaining a solution may be possible. Other alternative methods for phase control have also been demonstrated, as the application of a deformable mirror resulted in pulse shortening to 15 fs [18].

In conclusion, the numerical integration of Maxwell's equations for propagation of few-optical-cycle pulses in a dispersive Kerr medium shows a self-flattening effect of the pulse back front. From the calculated spectra and phase delay the possibility was predicted to extend the method of pulse shortening by SPM into the subcycle region.

We gratefully acknowledge support from the DFG, Project No. He2083/5-1, and partial support by BMBF, Project No. WEI-001-98. We thank Professor A. M. Weiner for a fruitful discussion of the physical limits of LCSLM's.

[1] G. P. Agrawal, *Nonlinear Fiber Optics* (Academic Press, New York, 1994).
[2] H. Nakatsuka, D. Grischkowsky, and A. C. Balant, Phys. Rev. Lett. **47**, 910 (1981); R. C. Fork *et al.*, Opt. Lett. **12**, 483 (1987).
[3] W. J. Tomlinson, R. H. Stolen, and C. V. Shank, J. Opt. Soc. Am. B **1**, 139 (1984).
[4] A. Baltuška *et al.*, Opt. Lett. **22**, 102 (1997).
[5] M. Nisoli *et al.*, Opt. Lett. **22**, 522 (1997).
[6] W. Zhao and E. Bourkoff, IEEE J. Quantum Electron. **24**, 365 (1988).
[7] G. Farcas and C. Toth, Phys. Lett. A **168**, 447 (1992); P. Antoine, A. L'Huillier, and M. Lewenstein, Phys. Rev. Lett. **77**, 1234 (1996); K. J. Schafer and K. C. Kulander, *ibid.* **78**, 638 (1997); I. P. Christov, M. M. Murnane, and H. C. Kapteyn, *ibid.* **78**, 1251 (1997).
[8] S. Yoshikawa and T. Imasaka, Opt. Commun. **96**, 94 (1993); A. E. Kaplan, Phys. Rev. Lett. **73**, 1243 (1994); S. E. Harris and A. V. Sokolov, *ibid.* **81**, 2894 (1998).
[9] V. P. Kalosha and J. Herrmann, Phys. Rev. Lett. **83**, 544 (1999).
[10] M. Sheik-Bahae *et al.*, IEEE J. Quantum Electron. **27**, 1296 (1991).
[11] K. S. Yee, IEEE Trans. Antennas Propag. **14**, 302 (1966); P. M. Goorjian *et al.*, IEEE J. Quantum Electron. **28**, 2416 (1992).
[12] *Handbook of Optical Constants*, edited by D. Palik (Academic Press, New York, 1985).
[13] M. Lenzner *et al.*, Phys. Rev. Lett. **80**, 4076 (1998); A. Tien *et al.*, *ibid.* **82**, 3883 (1999).
[14] R. G. Flesch, A. Pushkarev, and J. V. Moloney, Phys. Rev. Lett. **76**, 2488 (1996).
[15] M. Kempe *et al.*, J. Opt. Soc. Am. B **9**, 1158 (1992).
[16] A. M. Weiner, Prog. Quantum Electron. **19**, 161 (1995); A. M. Weiner, Rev. Sci. Instrum. (to be published).
[17] A. Efimov, C. Schafter, D. H. Reitze, J. Opt. Soc. Am. B **12**, 1968 (1995).
[18] E. Zeek *et al.*, Opt. Lett. **24**, 493 (1999).